Sixth Frequency Moment of the Frequency–Wave-Vector-Dependent Correlation Function for Isotropic Heisenberg Paramagnets at Elevated Temperatures

DANIEL G. MCFADDEN*† AND RAZA A. TAHIR-KHELI‡
Department of Physics, Temple University, Philadelphia, Pennsylvania 19122
(Received 28 August 1969)

We calculate the sixth frequency moment $\langle\omega^6\rangle_{\mathbf{K}}$ of the frequency–wave-vector-dependent spectral function for the isotropic Heisenberg paramagnet at elevated temperatures with arbitrary spin and arbitrary range of exchange interaction. These exact results are compared with the approximate sixth moment predicted by the two-parameter Gaussian representation used in the preceding paper for the generalized diffusivity. The general agreement of the approximate and the exact results for $\langle\omega^6\rangle_{\mathbf{K}}$ is satisfactory. For the exactly soluble spin-$\frac{1}{2}$ nearest-neighbor one-dimensional XY model, we compare the predictions of the two-parameter Gaussian approximation for $\langle\omega^6\rangle_{\mathbf{K}}{}^{zz}$ and $\langle\omega^8\rangle_{\mathbf{K}}{}^{zz}$ against the exact results for these moments (which are derived by using the corresponding exact spectral function given by Katsura *et al.* The agreement is again found to be satisfactory. This reinforces our confidence in the qualitative validity of the simple Gaussian approximation for the generalized diffusivity.

I. INTRODUCTION

As noted in the preceding paper,[1] the time dependence of the spin correlations is seemingly well described by a simple two-parameter Gaussian approximation[2] for the generalized diffusivity. An important check of the adequacy of any approximate frequency–wave-vector-dependent spectral function is a comparison of its frequency moments against the exact ones. The use of the appropriate two-parameter Gaussian approximation for the diffusivity automatically insures the exact preservation of the lowest three nontrivial frequency moments of the spectral function $F^{\alpha\alpha}(\mathbf{K},\omega)$, i.e., $\langle\omega^{2n}\rangle_{\mathbf{K}}{}^{\alpha\alpha}$ $n=0,1,2$. Therefore, one might ask how well such an approximate spectral function, constructed in the fashion described in Refs. 1 and 2, preserves the next most important[3] frequency moment, i.e., $\langle\omega^6\rangle_{\mathbf{K}}{}^{\alpha\alpha}$.

For the model system with only nearest-neighbor XY exchange and with $S=\frac{1}{2}$ spins distributed along a linear chain (i.e., the restricted XY model), the spectral function $F^{zz}(\mathbf{K},\omega)$ is exactly known.[4,5] From this, it is a simple matter to calculate the moments $\langle\omega^{2n}\rangle_{\mathbf{K}}{}^{zz}$ for all n. In Sec. II, we describe a comparison of the results for these moments for $n=3$ and 4, as obtained by using our approximate phenomenological theory (which uses only the knowledge of the moments with $n=0$, 1, and 2) and as computed from the exact results given in Ref. 4.

For the case of the isotropic Heisenberg paramagnet, only the zeroth, second, and fourth moments have been known until now (see the work of Marshall and coworkers in Ref. 3 and in the various works cited therein). Therefore, we have painstakingly carried out the computation of the sixth moment for this system. The labor involved in this effort is well over an order of magnitude more than that needed for computing all the three lower-order moments combined. The relevant algebra is inordinately long and tedious, and is in essence quite straightforward. We record the final results in Sec. III while some of the salient features of the calculation are relegated to an appendix. This result (for the sixth moment) is valid at elevated temperatures for general spin, arbitrary dimensionality, and for arbitrary range of the isotropic exchange interaction. We specialize it to a one-dimensional system with only nearest- and next–nearest-neighbor exchange, and record the comparison of the relevant approximate and exact sixth moments in Sec. IV.

Sections V and VI deal with two-dimensional (square net) and three-dimensional (simple cubic) lattices with nearest-neighbor exchange only.

The over-all agreement between the approximate and the exact sixth moments further reinforces our faith in the use of the phenomenological Gaussian representation for the diffusivity as a simple first approximation for studying the dynamical behavior of paramagnetic spin systems.

* Work forms part of a dissertation to be submitted to Temple University in partial fulfillment of the requirements of a Ph.D. degree.
† Supported by a National Science Foundation predoctoral fellowship.
‡ Supported by the U. S. Office of Naval Research.

[1] D. G. McFadden and R. A. Tahir-Kheli, preceding paper, Phys. Rev. **8**, 3649 (1970).

[2] R. A. Tahir-Kheli and D. G. McFadden, Phys. Rev. **178**, 800 (1969); **182**, 604 (1969).

[3] The reason the low-order frequency moments are relatively more important than the higher-order moments is that they are, in general, more sensitive to the detailed shape of the frequency–wave-vector-dependent spectral function in the region of small and intermediate frequencies. The dependence of the frequency moments upon the spectral function for large frequencies becomes rapidly more important as the order of the moment increases. Because the experimental measurements of the frequency spectrum are usually most reliable for low and intermediate frequencies [see W. Marshall and R. D. Lowde, in *Reports on Progress in Physics* (British Institute of Physics and the Physical Society, London, 1968), Vol. XXXI, Part II], therefore, it is reasonable to compare the exact result for the next–higher-order frequency moment to the approximate results.

[4] We have computed these moments for $n=3$ and 4 by using the appropriate exact result for the spectral function $F^{zz}(\mathbf{K},\omega)$, i.e., Eq. (55) in S. Katsura, T. Horiguchi, and M. Suzuki, Physica (to be published).

[5] T. Niemeijer, Physica **36**, 377 (1967).

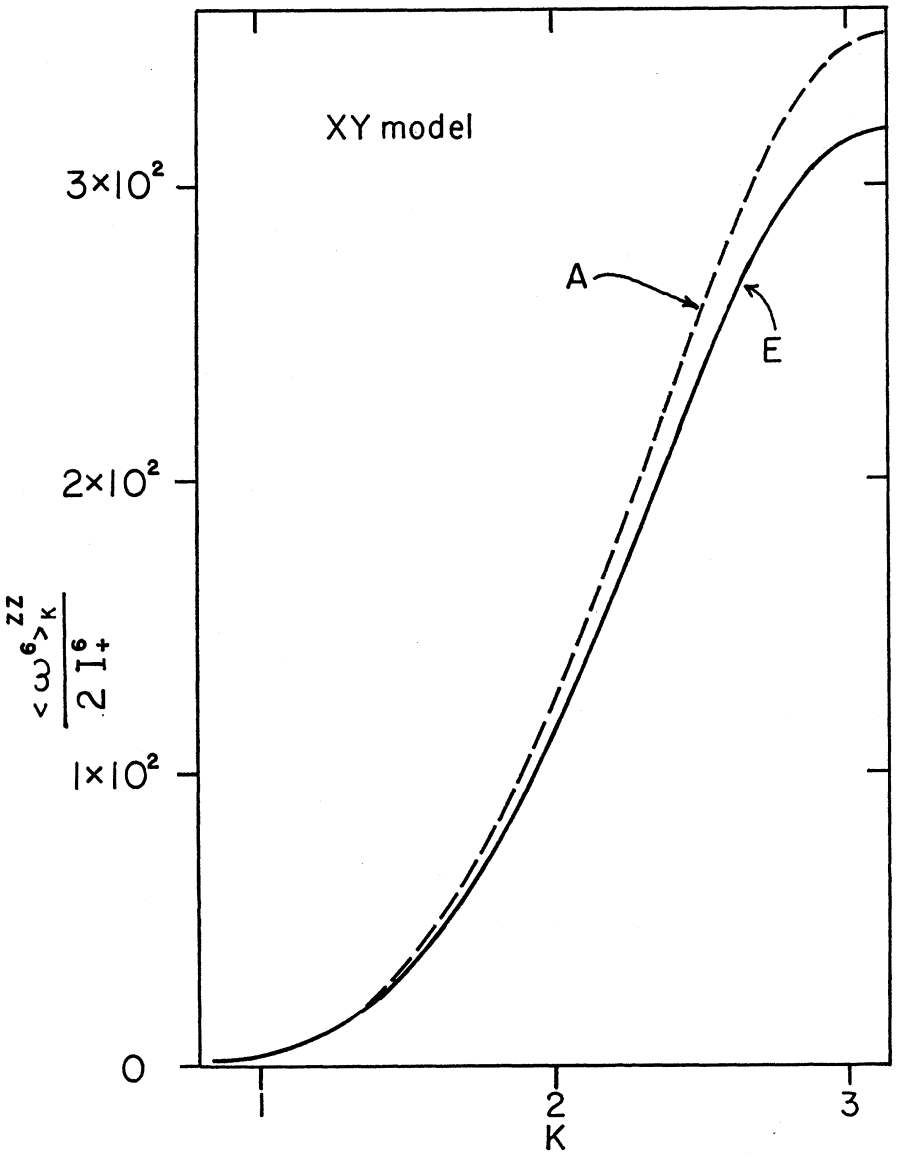

FIG. 1. Comparison of the approximate (A) and the exact (E) results for the sixth moment $\langle\omega^6\rangle_{\mathbf{K}}{}^{zz}$ as a function of the wave vector $\mathbf{K}$. The results refer to the restricted XY model, i.e., to a system of one-dimensional $S=\frac{1}{2}$ spins with only nearest-neighbor x-x and y-y exchange.

II. RESTRICTED XY MODEL

The exact solution for the longitudinal spectral function of the one-dimensional spin-$\frac{1}{2}$ XY model with only nearest-neighbor exchange, i.e.,

$$\begin{aligned} I_0(\mathbf{R})&=0 \quad \text{for all } \mathbf{R},\\ I_+(\mathbf{R})&=I_+ \quad \text{when } \mathbf{R} \text{ is equal to the nearest neighbor separation},\\ &=0 \quad \text{otherwise}, \end{aligned} \tag{2.1}$$

has been obtained by Katsura *et al.*[4,5] (The notation in the present paper is the same as that in the preceding one.) For our purposes, i.e., when $\beta I_+ \ll 1$, this may be written as follows:

$$\begin{aligned} [F^{zz}(\mathbf{K},\omega)]_{XY}&=(\tfrac{1}{2}\pi)\times[(4I_+\sin\tfrac{1}{2}K)^2-\omega^2]^{-1/2}\\ &\qquad \text{for } \omega<4I_+\sin\tfrac{1}{2}K,\\ &=0 \quad \text{otherwise}. \end{aligned} \tag{2.2}$$

This spectral function can readily be integrated to give the moments $\langle\omega^{2n}\rangle_{\mathbf{K}}{}^{zz}$. For $n=0$, 1, and 2, these moments are a special case of Eqs. (4.1a)–(4.1b) in the preceding paper. The appropriate sixth and eighth moments are as follows:

$$\langle\omega^6\rangle_{\mathbf{K}}{}^{zz}=640(I_+\sin\tfrac{1}{2}K)^6, \tag{2.3}$$

$$\langle\omega^8\rangle_{\mathbf{K}}{}^{zz}=8960(I_+\sin\tfrac{1}{2}K)^8. \tag{2.4}$$

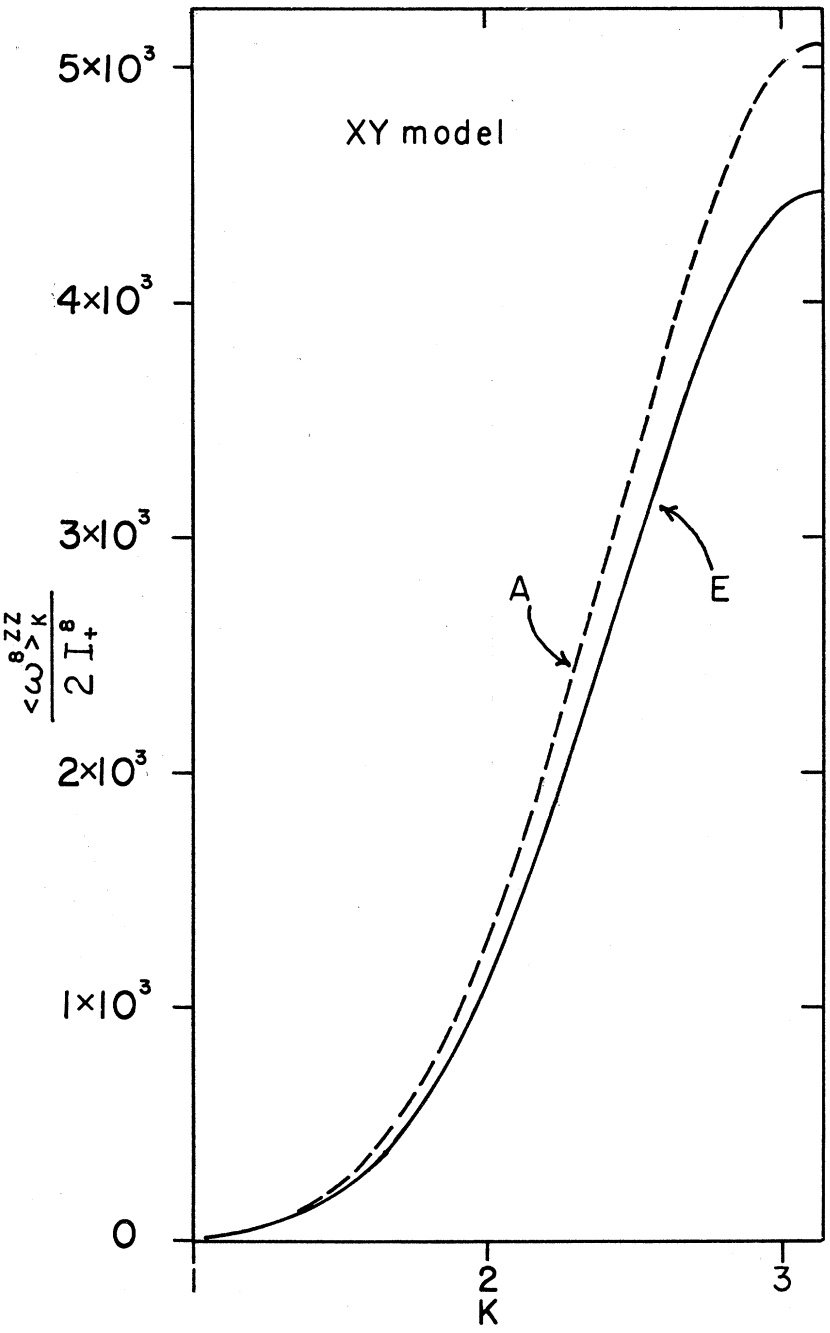

FIG. 2. Comparison of the exact (E) eighth moment $\langle\omega^8\rangle_K{}^{zz}$, with the corresponding approximate moment (A) obtained by using the two-parameter Gaussian representation for the diffusivity. These results refer to the restricted XY model.

On the basis of our approximate spectral function, we have computed approximate values of the sixth and eighth moments and compared them with the exact results (see Figs. 1 and 2).

The qualitative features of the two sets of results are strikingly similar. Even the quantitative agreement is fair.

III. SIXTH FREQUENCY MOMENT

The tedious calculation of the sixth frequency moment of the frequency–wave-vector-dependent spectral function for a Heisenberg paramagnet with isotropic exchange interactions of arbitrary range leads to the following result (see the discussion of the various salient features of this calculation in the

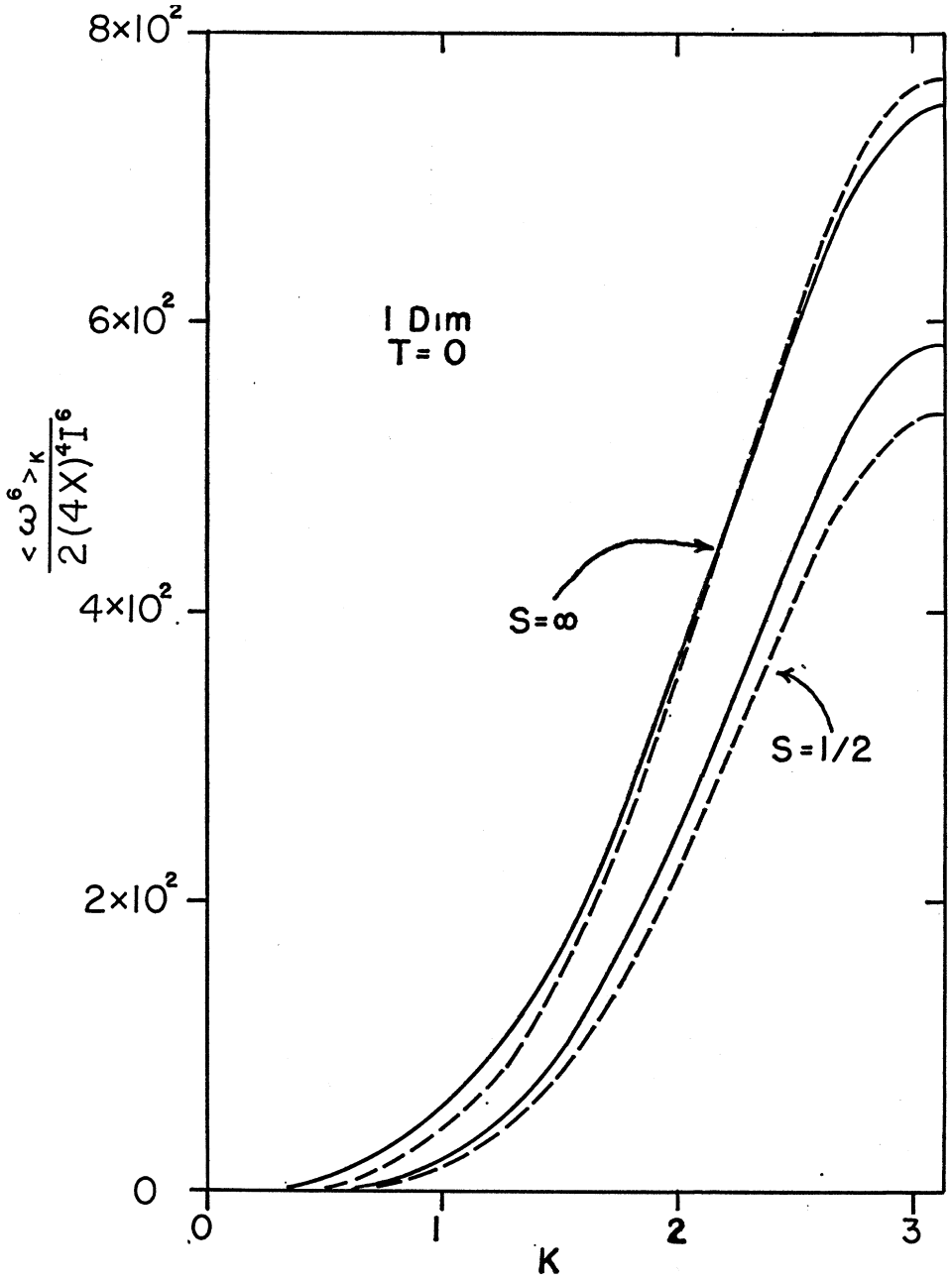

FIG. 3. Comparison of the exact (solid curves) and the approximate (dashed curves) sixth moment $\langle\omega^6\rangle_K=\langle\omega^6\rangle_K{}^{\alpha\alpha}$, $\alpha=x, y, z$, for a one-dimensional system of isotropically coupled Heisenberg spins (with only nearest-neighbor exchange) at elevated temperatures. The lower set of two curves refers to spin $\frac{1}{2}$, and the upper to spin ∞. Exact validity of the previously enunciated (see Refs. 1 and 2) empirical law of corresponding states would require the upper and lower set of curves to be identical. Similarly, a reasonable measure of the adequacy of our phenomenological two parameter theory is the size of the spread between the full and the dashed curves.

Appendix):

$$\langle\omega^6\rangle_K{}^{zz}=\langle\omega^6\rangle_K$$
$$=\frac{128}{5}X^2\sum_{\mathbf{R}}I^6(\mathbf{R})(1-e^{i\mathbf{K}\cdot\mathbf{R}})[342X^2-72X+31]$$
$$+128X^2\sum_{\mathbf{R}}\sum_{\mathbf{A}}\{[I(\mathbf{R})I(\mathbf{A})]^3[\tfrac{4}{5}X^2(27-46e^{i\mathbf{K}\cdot\mathbf{R}}+19e^{i\mathbf{K}\cdot(\mathbf{R}-\mathbf{A})})$$
$$+(8/5)X(4-7e^{i\mathbf{K}\cdot\mathbf{R}}+3e^{i\mathbf{K}\cdot(\mathbf{R}-\mathbf{A})})+\tfrac{2}{5}(-3+4e^{i\mathbf{K}\cdot\mathbf{R}}-e^{i\mathbf{K}\cdot(\mathbf{R}-\mathbf{A})})]$$

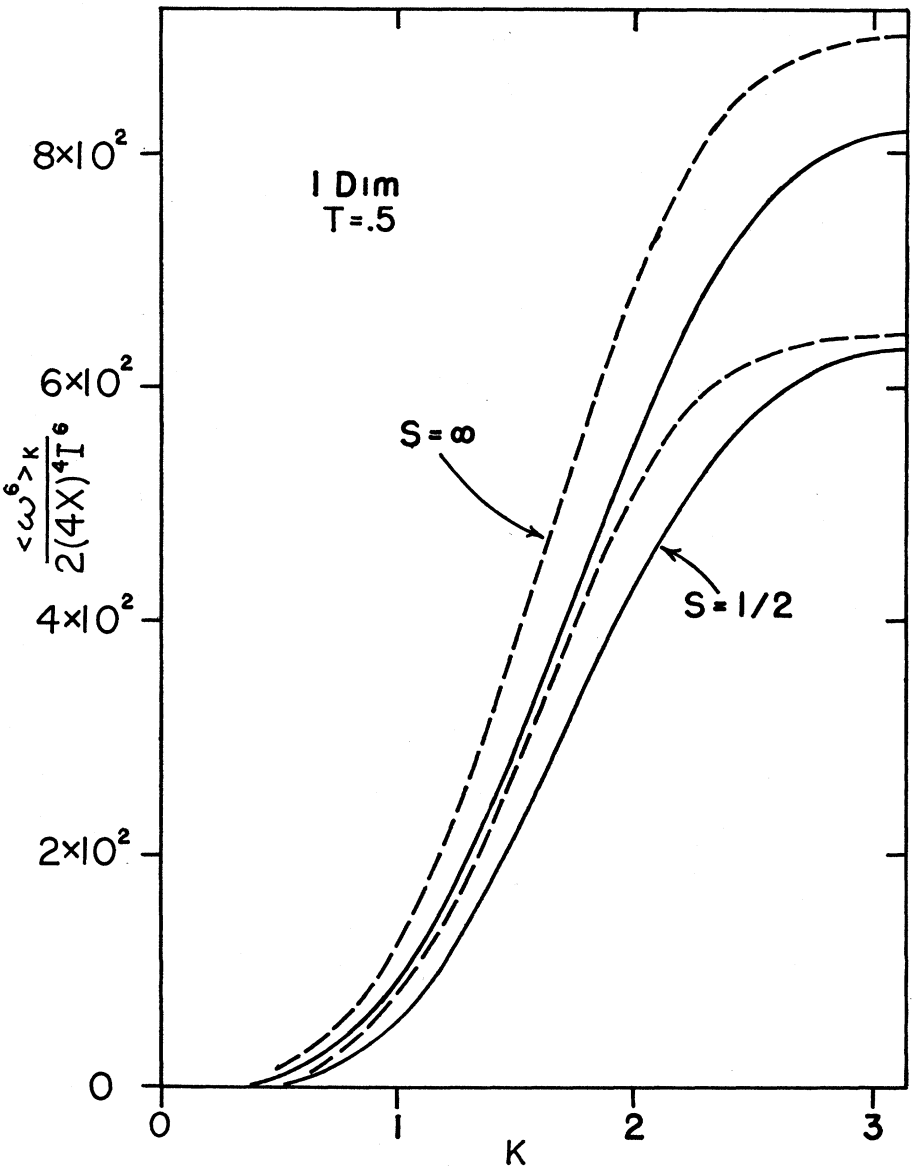

FIG. 4. Plot of the exact (solid) and the approximate (dashed) infinite-temperature sixth moment for a one-dimensional isotropic Heisenberg spin system. This plot corresponds to the case for which the ratio of the second-nearest to the nearest-neighbor exchange is equal to $\frac{1}{2}$. The lower set of curves correspond to spin $\frac{1}{2}$, and the upper to spin ∞. This plot should be compared to Fig. 3, which corresponds to $T=0$.

$$+I^4(\mathbf{R})I^2(\mathbf{A})[(16/5)X^2(-68+55e^{i\mathbf{K}\cdot\mathbf{R}}+32e^{i\mathbf{K}\cdot\mathbf{A}}-19e^{i\mathbf{K}\cdot(\mathbf{R}-\mathbf{A})})$$
$$+X(-17+(93/5)e^{i\mathbf{K}\cdot\mathbf{R}}-e^{i\mathbf{K}\cdot\mathbf{A}}-\tfrac{3}{5}e^{i\mathbf{K}\cdot(\mathbf{R}-\mathbf{A})})+\tfrac{4}{5}(-3+2e^{i\mathbf{K}\cdot\mathbf{R}}+2e^{i\mathbf{K}\cdot\mathbf{A}}-e^{i\mathbf{K}\cdot(\mathbf{R}-\mathbf{A})})]$$
$$+I^4(\mathbf{R})I(\mathbf{A})I(\mathbf{R}-\mathbf{A})[8X^2(-1+(31/5)e^{i\mathbf{K}\cdot\mathbf{R}}-(26/5)e^{i\mathbf{K}\cdot\mathbf{A}})$$
$$+\tfrac{1}{5}X(79-87e^{i\mathbf{K}\cdot\mathbf{R}}+8e^{i\mathbf{K}\cdot\mathbf{A}})+\tfrac{2}{5}(-3+5e^{i\mathbf{K}\cdot\mathbf{R}}-2e^{i\mathbf{K}\cdot\mathbf{A}})]$$
$$+I^3(\mathbf{R})I^2(\mathbf{A})I(\mathbf{R}-\mathbf{A})[8X^2(3-(71/5)e^{i\mathbf{K}\cdot\mathbf{R}}+7e^{i\mathbf{K}\cdot\mathbf{A}}+(21/5)e^{i\mathbf{K}\cdot(\mathbf{R}-\mathbf{A})})$$
$$+2X(-(16/5)+(8/5)e^{i\mathbf{K}\cdot\mathbf{R}}+15e^{i\mathbf{K}\cdot\mathbf{A}}-(67/5)e^{i\mathbf{K}\cdot(\mathbf{R}-\mathbf{A})})+\tfrac{2}{5}(6-3e^{i\mathbf{K}\cdot\mathbf{R}}-5e^{i\mathbf{K}\cdot\mathbf{A}}+2e^{i\mathbf{K}\cdot(\mathbf{R}-\mathbf{A})})]$$
$$+[I(\mathbf{R})I(\mathbf{A})I(\mathbf{R}-\mathbf{A})]^2(e^{i\mathbf{K}\cdot\mathbf{R}}-1)(2X-12X^2)\}$$

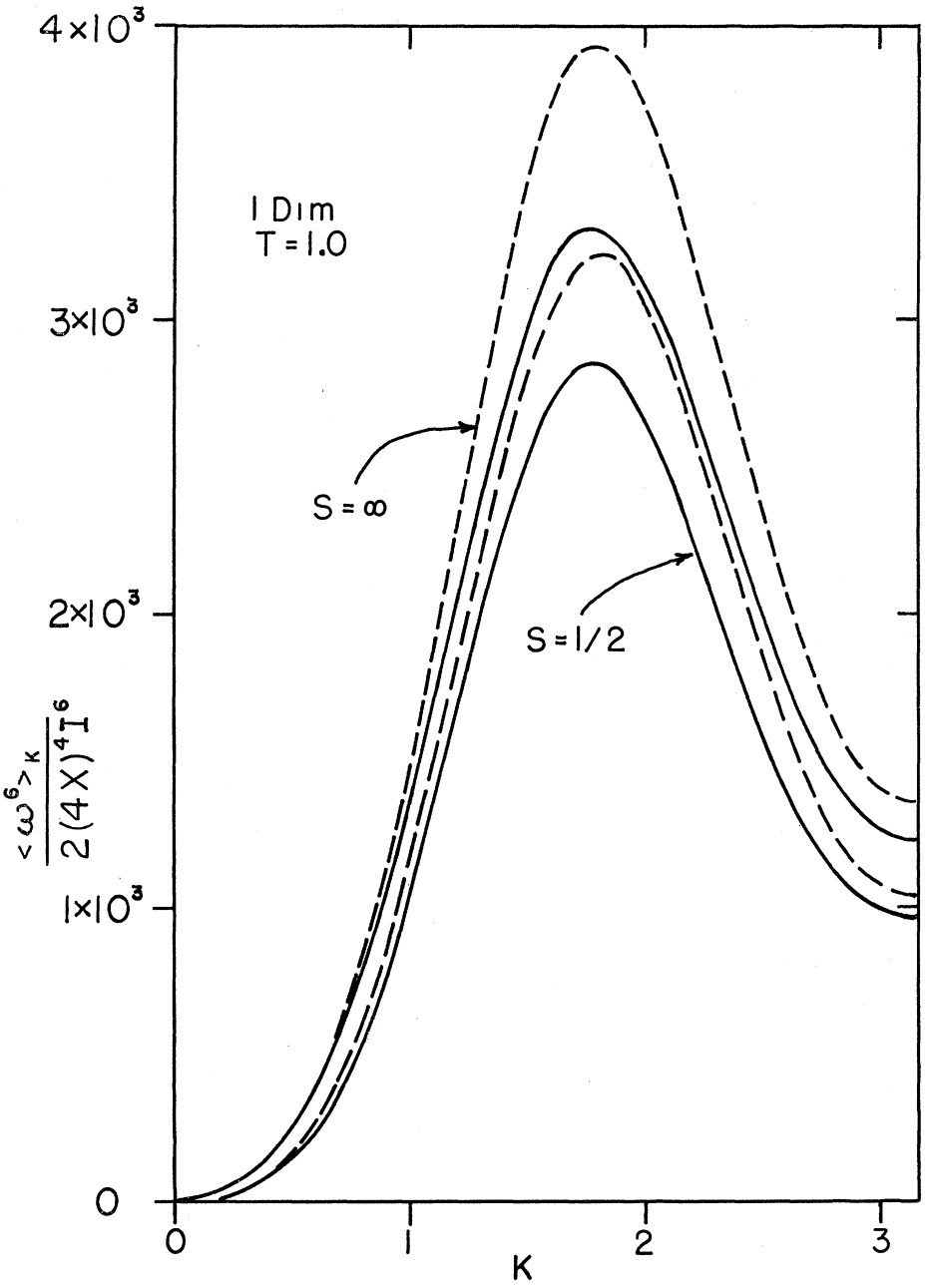

FIG. 5. Comparison of the exact (solid curves) and the approximate (dashed curves) sixth frequency moments with $T=1$. The lower set of curves correspond to spin $\frac{1}{2}$, and the upper to spin ∞.

$$+256X^4\sum_{\mathbf{A}}\sum_{\mathbf{B}}\sum_{\mathbf{R}}\{[I(\mathbf{R})I(\mathbf{A})I(\mathbf{B})]^2(97-152e^{i\mathbf{K}\cdot\mathbf{R}}+65e^{i\mathbf{K}\cdot(\mathbf{R}+\mathbf{A})}-10e^{i\mathbf{K}\cdot(\mathbf{R}+\mathbf{A}+\mathbf{B})})$$

$$+[I(\mathbf{R})I(\mathbf{A})]^2I(\mathbf{B})I(\mathbf{R}+\mathbf{A}+\mathbf{B})(-7-30e^{i\mathbf{K}\cdot(\mathbf{R}+\mathbf{B})}+15e^{i\mathbf{K}\cdot(\mathbf{R}+\mathbf{A})}-6e^{i\mathbf{K}\cdot\mathbf{B}}+28e^{i\mathbf{K}\cdot\mathbf{A}})$$

$$+I(\mathbf{R})I(\mathbf{A})I(\mathbf{B})I(\mathbf{R}-\mathbf{A})I(\mathbf{R}-\mathbf{B})I(\mathbf{A}-\mathbf{B})(2e^{i\mathbf{K}\cdot\mathbf{R}}-2)$$

$$+[I(\mathbf{R})I(\mathbf{A})]^2I(\mathbf{B})I(\mathbf{R}+\mathbf{B})(-74+10e^{i\mathbf{K}\cdot(\mathbf{R}+\mathbf{A})}-32e^{i\mathbf{K}\cdot(\mathbf{A}+\mathbf{B})}$$

$$+14e^{i\mathbf{K}\cdot(\mathbf{R}+\mathbf{B})}+2e^{i\mathbf{K}\cdot(\mathbf{R}+\mathbf{A}+\mathbf{B})}+28e^{i\mathbf{K}\cdot\mathbf{A}}+104e^{i\mathbf{K}\cdot\mathbf{B}}-52e^{i\mathbf{K}\cdot\mathbf{R}})$$

$$+I^2(\mathbf{R})I(\mathbf{A})I(\mathbf{B})I(\mathbf{R}-\mathbf{A})I(\mathbf{A}-\mathbf{B})(26+12e^{i\mathbf{K}\cdot(\mathbf{R}-\mathbf{A})}-18e^{i\mathbf{K}\cdot(\mathbf{R}-\mathbf{B})}-6e^{i\mathbf{K}\cdot\mathbf{B}}-18e^{i\mathbf{K}\cdot\mathbf{A}}+4e^{i\mathbf{K}\cdot\mathbf{R}})$$

$$+I^2(\mathbf{R})I(\mathbf{A})I(\mathbf{B})I(\mathbf{R}-\mathbf{A})I(\mathbf{R}-\mathbf{B})(-10-2e^{i\mathbf{K}\cdot(\mathbf{A}-\mathbf{B})}+18e^{i\mathbf{K}\cdot\mathbf{A}}-6e^{i\mathbf{K}\cdot\mathbf{R}})\}, \quad (3.1)$$

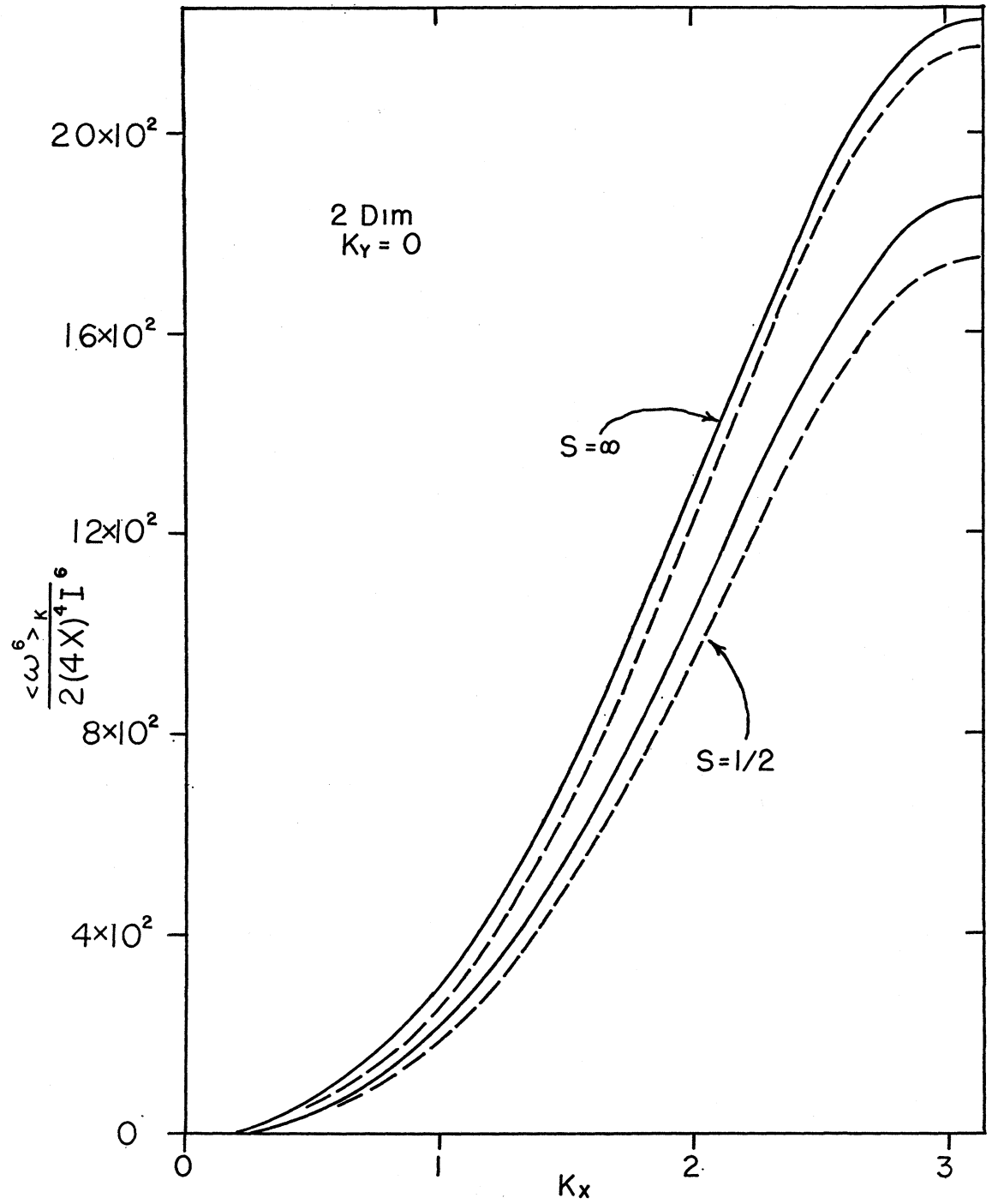

FIG. 6. The exact (solid curves) and the approximate (dashed curves) for the sixth frequency moment of the spectral function for a two-dimensional (square net) lattice of isotropic Heisenberg spins with only nearest-neighbor exchange equal to I. The $\mathbf{K}$ vector is taken to be along the x direction. The lower set of curves refers to spin $\frac{1}{2}$, and the upper to spin ∞.

where

$$X=\tfrac{1}{3}S(S+1). \tag{3.2}$$

The superscripts are dispensed with at this point, since we are treating an isotropic system. The above result holds only in the limit of elevated temperatures. In the relevant Hamiltonian, i.e.,

$$\mathcal{H}=-\sum_{g,f} I(g,f)S_f\cdot S_g, \tag{3.3}$$

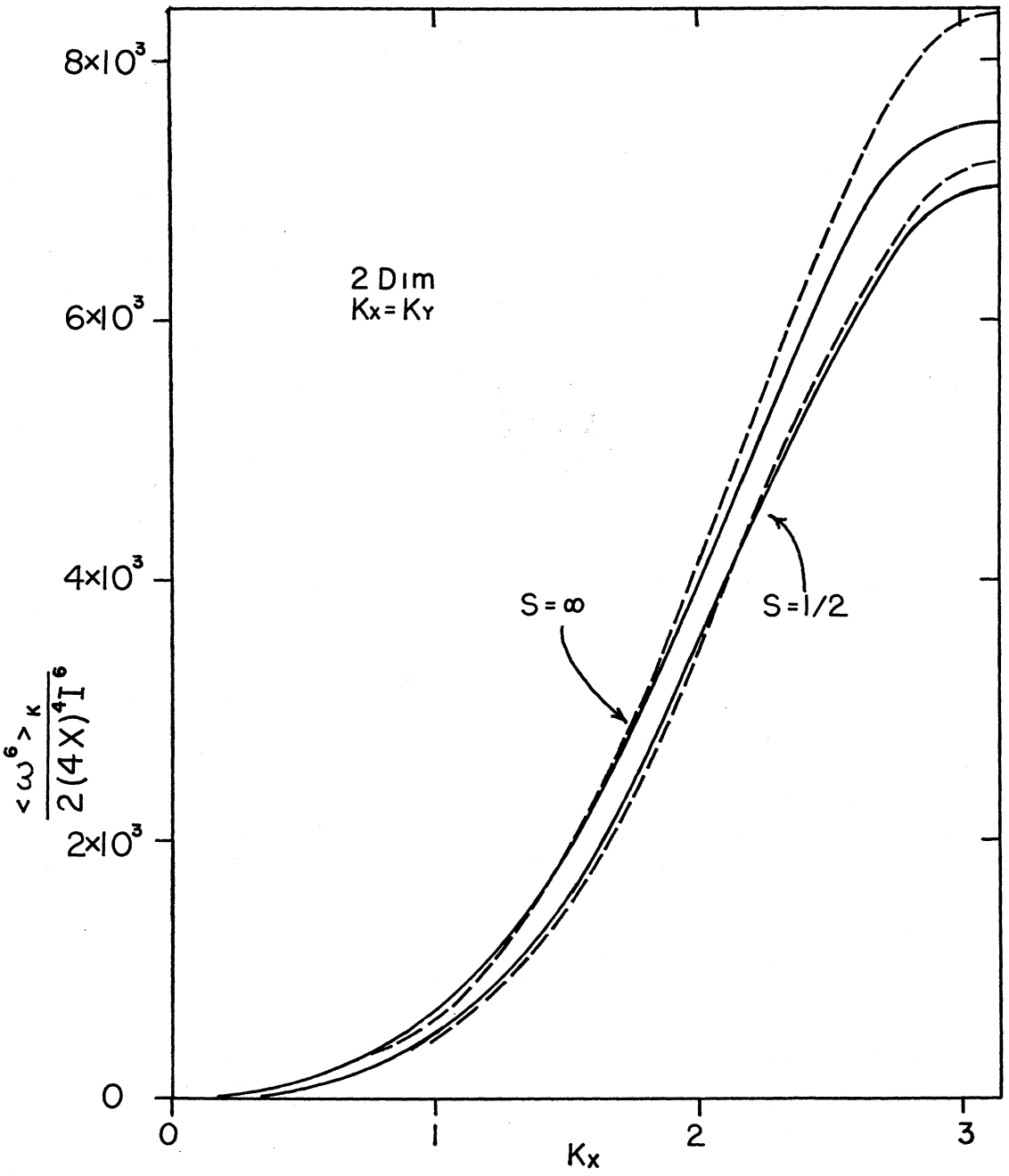

FIG. 7. The legend is the same as in Fig. 6 except for the fact that the **K** vector, i.e., $\mathbf{K}=\hat{\imath}K_x+\hat{\jmath}K_y$, is now taken to be along the diagonal $K_x=K_y$. Note that there is somewhat better agreement between the approximate and exact results in two dimensions than in one dimension.

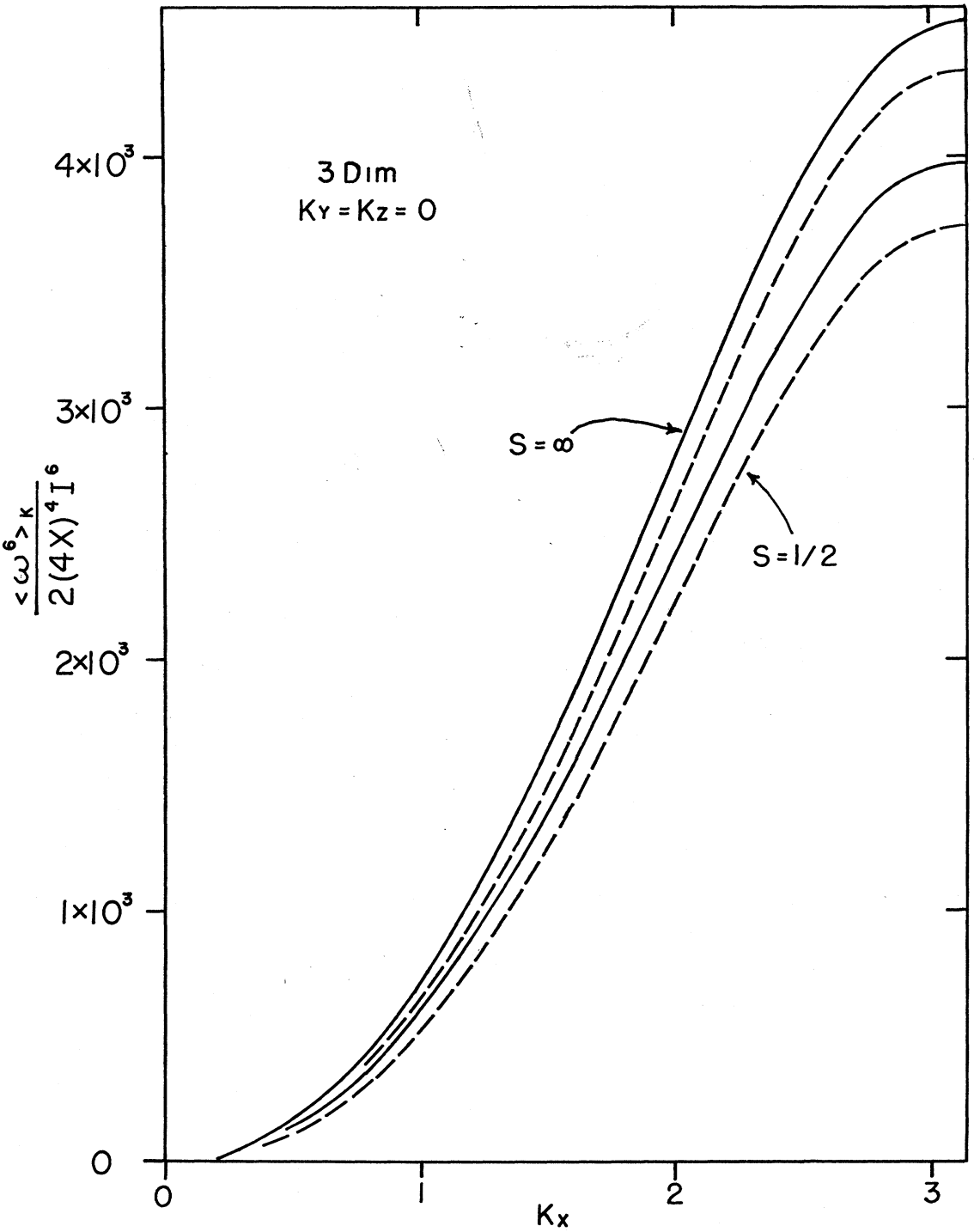

FIG. 8. Plot of the exact (solid curves) and the approximate (dashed curves) for the sixth frequency moment of the frequency–wave-vector-dependent spectral function of a three-dimensional (simple cubic) lattice of isotropic Heisenberg spins with only nearest-neighbor exchange. The lower curves correspond to the case of spin $\frac{1}{2}$, and the upper to spin ∞. The **K** vector is taken to be along the [100] direction.

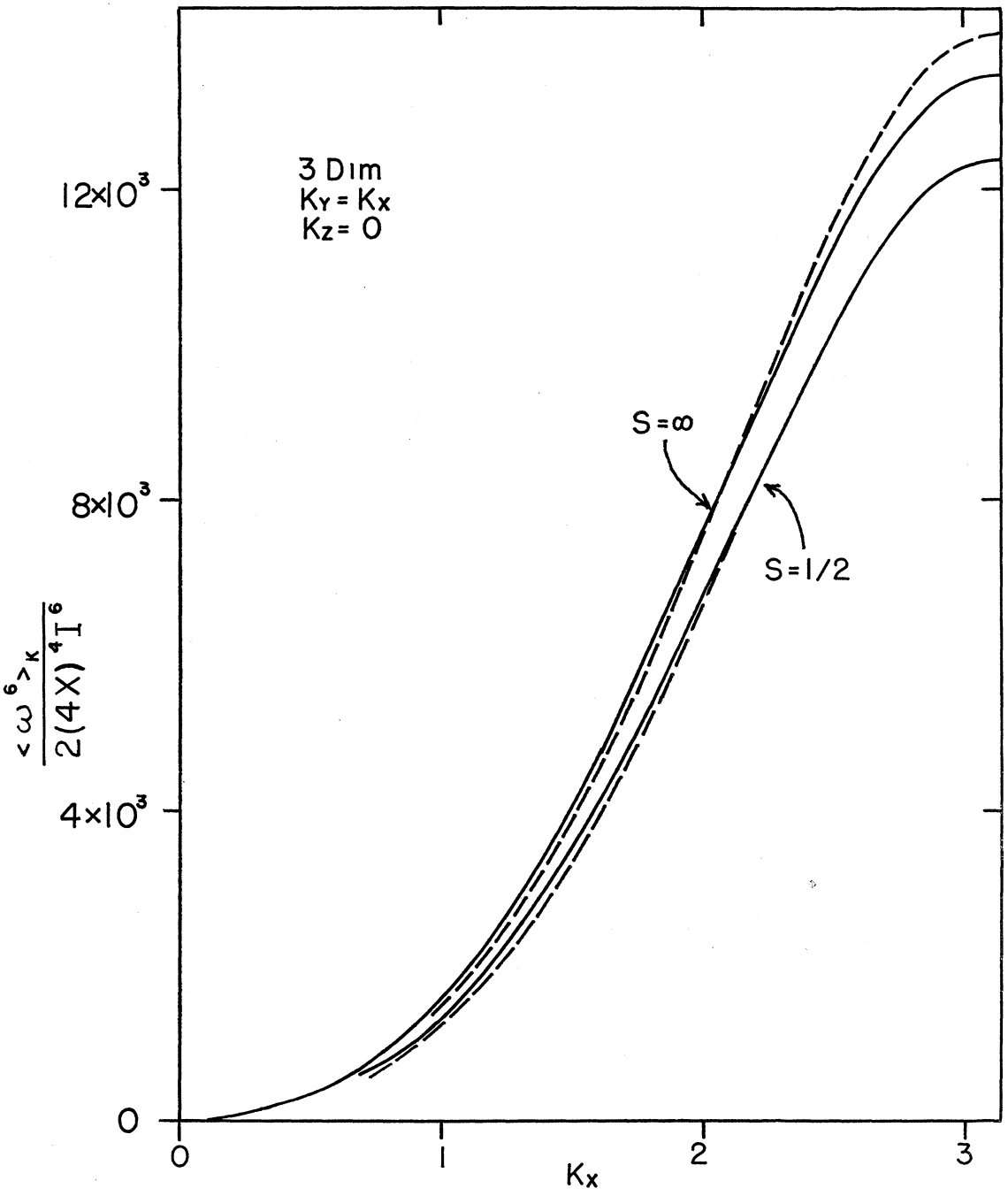

FIG. 9. The legend is the same as in Fig. 8, the only difference being that now the **K** vector is along the [110] direction.

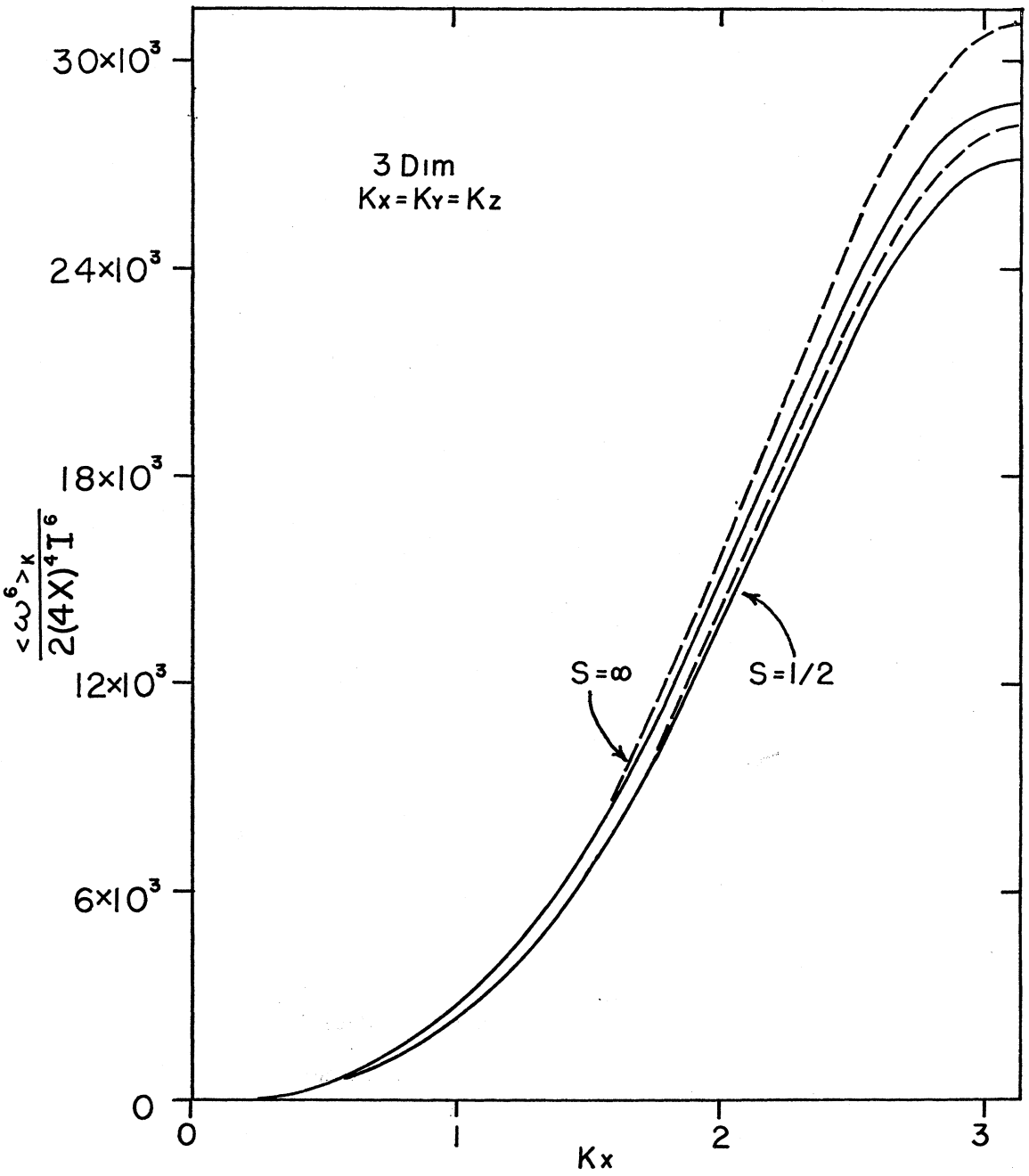

FIG. 10. The legend is the same as in Figs. 8 and 9, the only difference being that now the **K** vector is along the [111] direction.

the range of the exchange interaction is taken to be arbitrary. Note that the magnitude of the spin S and the dimensionality of the lattice are arbitrary.

IV. RESULTS IN ONE DIMENSION

To do calculations with the sixth moment as given in Eq. (3.1), it is necessary to specialize it to the lattice structure in question and to explicitly specify the spatial structure of the exchange interaction.

For a linear chain with nearest-neighbor $[I(1)]$ and next-nearest-neighbor $[I(2)]$ exchange, the result for

the sixth moment is as follows:

$$\langle\omega^6\rangle_K/2I(1)^6=(4X)^4[(1-C_1)(951/5-722C_1/5+40C_1^2)+T(1-C_1)(-498-288C_1+120C_1^2)$$
$$+T^2(1374-6286C_1/5-3916C_1^2/5+4792C_1^3/5-240C_1^4-52C_3)$$
$$+T^3(-3936/5+478C_1/5+4644C_1^2/5+104C_1^3/5-240C_1^4-18C_3)$$
$$+T^4(10488/5-4258C_1/5-15672C_1^2/5+6392C_1^3/5+1120C_1^4-480C_1^5-30C_3)$$
$$+T^6(3821/5-8834C_1^2/5+6688C_1^4/5-320C_1^6-15C_4)]$$
$$+(128/5)X^3(1-C_1)[-42C_1-178+252T(1+C_1)+T^2(-382-288C_1+12C_1^2)+192T^3(1-C_1^2)$$
$$+T^4(-190-186C_1+12C_1^2)+T^6(1+C_1)(-272-168C_1^2)]$$
$$+(256/5)X^2(1-C_1)[-\tfrac{5}{2}+6C_1+T^2(-9+2C_1+8C_1^2)+T^3(-11-2C_1+8C_1^2)$$
$$+T^4(-28-18C_1+8C_1^2)+T^6(-17-24C_1^2)(1+C_1)]. \quad (4.1)$$

In the above equation, we have used the notation

$$C_n=\cos(nK), \quad T=I(2)/I(1). \quad (4.2)$$

The above exact result is plotted as solid curves in Figs. 3–5 for spin $\frac{1}{2}$ and spin ∞. T, the ratio of the next-nearest-neighbor to nearest-neighbor exchange, is taken to be equal to 0, 0.5, and 1.0, respectively, in Figs. 3–5.

To compare the exact results with those given by the approximate spectral function (constructed by using the two-parameter Gaussian representation for the diffusivity), we have computed the approximate sixth moment and plotted the results as dashed curves in the same figures. The discrepancy between the approximate and the exact sixth moments gives a measure of the adequacy of the approximate spectral function derived in Refs. 1 and 2. Similarly, the spread between the $S=\frac{1}{2}$ and the $S=\infty$ curves reflects upon the usefulness of the empirical law of corresponding states enunciated in Refs. 1 and 2.

V. RESULTS IN TWO DIMENSIONS

For brevity, we shall study only the case of nearest-neighbor exchange for a square lattice. The appropriate representation of the sixth moment for this system is found to be

$$\langle\omega^6\rangle_K/2I(1)^6=256X^4(2-C)(5971/5-1972C/5+40C^2)$$
$$+512X^4(-108-15C_x^2-15C_y^2-60C_xC_y+99C)+(128/5)X^2(2-C)[X(-284-42C)+12C-41]. \quad (5.1)$$

In the above equation, we have used the notation

$$C_x=\cos K_x, \quad C_y=\cos K_y, \quad C=C_x+C_y. \quad (5.2)$$

We have plotted the above exact, and the appropriate approximate, results for the sixth moment in Figs. 6 and 7. The relative fit of the various results is seen to be a strong function of the magnitude of the **K** vector (as was the case in one dimension) as well as its direction. For example, the approximate (dashed) curves cross over the exact (solid) curves in Fig. 7, which refers to the case for which the **K** vector is along the diagonal to the x and the y axes. On the other hand, the same curves do not cross over in Fig. 6, which refers to the case where **K** is along the x axis.

VI. RESULTS IN THREE DIMENSIONS

Again, for brevity and convenience, we examine only the simplest three-dimensional lattice, the simple cubic, and assume the range of the exchange interactions to be limited to the nearest neighbor. The corresponding result for the sixth moment is

$$\langle\omega^6\rangle_K/2I(1)^6=256X^4(3-C)(14691/5-3072C/5+40C^2)$$
$$+512X^4[-270-60(C_xC_y+C_xC_z+C_yC_z)-15(C_x^2+C_y^2+C_z^2)+165C]$$
$$+(128/5)(3-C)X^2[-X(390+42C)-77+12C]. \quad (6.1)$$

In the above equation, we have used the notation

$$C_x=\cos(K_x), \quad C_y=\cos(K_y),$$
$$C_z=\cos(K_z), \quad C=C_x+C_y+C_z. \quad (6.2)$$

In Figs. 8–10, we have plotted the above exact results, as well as the corresponding approximate results obtained by using the phenomenological construct for the spectral function.

The general features of the results are found to be not unlike those obtained for one and two dimensions.

ACKNOWLEDGMENT

We are greatly indebted to the Temple University computer center for the generous allotment of computer time on their CDC-6400.

APPENDIX

In a calculation as long and as tedious as the one described in this paper, it is very important to devise checks that the various intermediate steps can be subjected to. The most efficient procedure for calculating the sixth moment $\langle\omega^6\rangle_{\mathbf{K}}$ is to start with the identity

$$\lim_{\beta\to 0}\langle\omega^6\rangle_{\mathbf{K}}=2\sum_{(g-w)}e^{-i\mathbf{K}(g-w)}\times\left\langle\left(i\frac{d}{dt}\right)^3 S_g^z(t)\left(-i\frac{d}{dt'}\right)^3 S_w^z(t')\right\rangle_{t=t'}. \tag{A1}$$

[Compare with Eq. (2.8b) of the preceding paper.] The reason for this is that here we only need to calculate $(i\,d/dt)^3 S_g^z(t)$, because quite obviously if

$$\left(i\frac{d}{dt}\right)^n S_g^z(t)=\rho_g^{(n)}(t), \tag{A2}$$

then

$$\left(-i\frac{d}{dt}\right)^n S_g^z(t)=(-1)^n\rho_g^{(n)}(t). \tag{A3}$$

Moreover, since the calculation of the repeated commutators with the Hamiltonian, i.e., $(i\,d/dt)^n S_g^z(t)$, becomes rapidly more cumbersome the as order n of the repetition increases, therefore, the most efficient calculation for the sixth moment is via the identity (1).

Under the Hamiltonian (3.2), we find $\rho_g^{(3)}(t)$. Then we recast it into the following convenient form:

$$-\rho_g^{(3)}(t)=A_g+B_g+C_g+D_g+E_g+F_g+G_g+H_g, \tag{A4}$$

where

$$\begin{aligned}
A_g=&4\sum_{f,m,i}[I(gm)I(fm)(1-\delta_{gf})-I(gf)I(fm)(1-\delta_{gm})-I(gf)I(gm)(1-\delta_{fm})]\\
&\times[I(gi)S_f^zS_g^z(S_i^+S_m^--S_m^+S_i^-)(1-\delta_{if})+I(im)S_f^zS_m^z(S_i^+S_g^--S_g^+S_i^-)(1-\delta_{if})\\
&+I(im)S_f^zS_i^z(S_g^+S_m^--S_m^+S_g^-)(1-\delta_{if})(1-\delta_{ig})+I(gi)S_f^zS_i^z(S_m^+S_g^--S_g^+S_m^-)(1-\delta_{if})(1-\delta_{im})]\\
&+8\sum_{f,m,i}[I(gf)-I(gi)]I(gm)I(if)S_g^zS_f^z(S_i^+S_m^--S_m^+S_i^-)(1-\delta_{gf})(1-\delta_{gi})(1-\delta_{fm}),
\end{aligned} \tag{A5a}$$

$$\begin{aligned}
B_g=&2\sum_{f,m,i}[I(gm)I(fm)(1-\delta_{gf})-I(gf)I(fm)(1-\delta_{gm})-I(gf)I(gm)(1-\delta_{fm})]\\
&\times I(if)(S_f^+S_i^--S_i^+S_f^-)(S_g^+S_m^-+S_m^+S_g^-)(1-\delta_{ig})(1-\delta_{im})\\
&+4\sum_{f,m,i}I(gf)I(gm)I(gi)(S_g^+S_i^--S_i^+S_g^-)S_f^+S_m^-(1-\delta_{if})(1-\delta_{im})(1-\delta_{fm}),
\end{aligned} \tag{A5b}$$

$$\begin{aligned}
C_g=&4\sum_{f,m}I(gm)I(gm)\{[4I(gf)-I(fm)]S_m^zS_g^z(S_g^+S_f^--S_f^+S_g^-)(1-\delta_{fm})+I(gf)S_g^zS_m^z(S_m^+S_f^--S_f^+S_m^-)\\
&+[I(fm)(1-\delta_{gf})-I(gf)(1-\delta_{fm})]S_m^zS_f^z(S_m^+S_g^--S_g^+S_m^-)\\
&+[I(fm)(1-\delta_{gf})-I(gf)(1-\delta_{fm})]S_g^zS_f^z(S_g^+S_m^--S_m^+S_g^-)-2I(gf)S_m^zS_g^+S_f^-(1-\delta_{fm})\\
&-I(gf)S_g^z(S_m^+S_f^-+S_f^+S_m^-)(1-\delta_{fm})+I(fm)S_m^z(S_g^+S_f^-+S_f^+S_g^-)(1-\delta_{gf})\\
&+[I(gf)-I(fm)]S_f^z(S_g^+S_m^-+S_m^+S_g^-)(1-\delta_{gf})(1-\delta_{fm})\}\\
&+4\sum_{f,m}[I(gm)I(fm)(1-\delta_{gf})-I(gf)I(fm)(1-\delta_{gm})-I(gf)I(gm)(1-\delta_{fm})]\\
&\times[I(gf)S_f^zS_g^z(S_f^+S_m^--S_m^+S_f^-)+I(fm)S_f^zS_m^z(S_f^+S_g^--S_g^+S_f^-)\\
&+I(gm)S_f^zS_g^z(S_g^+S_m^--S_m^+S_g^-)+I(gm)S_f^zS_m^z(S_m^+S_g^--S_g^+S_m^-)]\\
&-4\sum_{f,m}[I(gm)I(fm)-I(gf)I(fm)-I(gf)I(gm)]I(gm)S_f^z(S_g^+S_m^-+S_m^+S_g^-)(1-\delta_{gf})(1-\delta_{fm})\\
&+8\sum_{f,m}[I(gf)-I(gm)]I(gf)I(mf)S_g^zS_f^z(S_m^+S_f^--S_f^+S_m^-)(1-\delta_{gm})\\
&+8\sum_{f,m}[I(gf)-I(gm)]I(gf)I(fm)S_g^zS_f^+S_m^-(1-\delta_{gm}),
\end{aligned} \tag{A5c}$$

$$\begin{aligned}
D_g=&2\sum_{f,m}I(gm)I(gm)[I(fm)(S_f^+S_m^-S_g^+S_m^--S_m^+S_f^-S_m^+S_g^-)(1-\delta_{gf})\\
&+I(gf)(S_g^+S_f^-S_g^+S_m^--S_f^+S_g^-S_m^+S_g^-)(1-\delta_{fm})+2I(gf)(S_g^+S_m^-S_f^+S_m^--S_m^+S_g^-S_m^+S_f^-)(1-\delta_{fm})]\\
&+2\sum_{f,m}[I(gm)I(fm)(1-\delta_{gf})-I(gf)I(fm)(1-\delta_{gm})-I(gf)I(gm)(1-\delta_{fm})]\\
&\times[I(gf)(S_f^+S_g^-S_m^+S_g^--S_g^+S_f^-S_g^+S_m^-)+I(fm)(S_f^+S_m^-S_g^+S_m^--S_m^+S_f^-S_m^+S_g^-)],
\end{aligned} \tag{A5d}$$

$$E_g=2\sum_{f,m} I(gm)I(gm)[2I(fm)(S_f{}^+S_m{}^- - S_m{}^+S_f{}^-)S_g{}^+S_g{}^-(1-\delta_{gf})$$
$$+2I(fm)S_m{}^zS_m{}^z(S_g{}^+S_f{}^- - S_f{}^+S_g{}^-)+I(fm)(S_f{}^+S_m{}^-S_m{}^+S_g{}^- - S_m{}^+S_f{}^-S_g{}^+S_m{}^-)(1-\delta_{gf})$$
$$+6I(gf)S_g{}^zS_g{}^z(S_f{}^+S_m{}^- - S_m{}^+S_f{}^-)+I(gf)(S_g{}^+S_f{}^-S_m{}^+S_g{}^- - S_f{}^+S_g{}^-S_g{}^+S_m{}^-)(1-\delta_{fm})$$
$$+2I(gf)(S_g{}^+S_m{}^-S_m{}^+S_f{}^- - S_m{}^+S_g{}^-S_f{}^+S_m{}^-)(1-\delta_{fm})+2I(gf)(S_g{}^+S_f{}^- - S_f{}^+S_g{}^-)S_m{}^+S_m{}^-(1-\delta_{fm})]$$
$$+2\sum_{f,m}[I(gm)I(fm)(1-\delta_{gf})-I(gf)I(fm)(1-\delta_{gm})-I(gf)I(gm)(1-\delta_{fm})]$$
$$\times[I(gf)(S_f{}^+S_g{}^-S_g{}^+S_m{}^- - S_g{}^+S_f{}^-S_m{}^+S_g{}^-)+I(mf)(S_f{}^+S_m{}^-S_m{}^+S_g{}^- - S_m{}^+S_f{}^-S_g{}^+S_m{}^-)$$
$$+2I(mf)S_f{}^zS_f{}^z(S_g{}^+S_m{}^- - S_m{}^+S_g{}^-)+2I(gf)S_f{}^zS_f{}^z(S_m{}^+S_g{}^- - S_g{}^+S_m{}^-)], \quad \text{(A5e)}$$

$$F_g=4\sum_m [I(gm)]^3[(S_g{}^+S_m{}^- - S_m{}^+S_g{}^-)S_g{}^+S_g{}^- + S_m{}^zS_m{}^z(S_g{}^+S_m{}^- - S_m{}^+S_g{}^-)$$
$$+S_g{}^zS_g{}^z(S_g{}^+S_m{}^- - S_m{}^+S_g{}^-)-2S_g{}^zS_g{}^+S_m{}^- + 2S_m{}^zS_m{}^+S_g{}^- + 2S_g{}^zS_m{}^z(S_g{}^+S_m{}^- - S_m{}^+S_g{}^-)$$
$$+(S_g{}^+S_m{}^- - S_m{}^+S_g{}^-)S_m{}^+S_m{}^- + S_g{}^+S_m{}^- - S_m{}^+S_g{}^-], \quad \text{(A5f)}$$

$$G_g=4\sum_m [I(gm)]^3(S_g{}^+S_m{}^-S_g{}^+S_m{}^- - S_m{}^+S_g{}^-S_m{}^+S_g{}^-), \quad \text{(A5g)}$$

$$H_g=4\sum_m [I(gm)]^3[S_g{}^+S_m{}^-S_m{}^+S_g{}^- - S_m{}^+S_g{}^-S_g{}^+S_m{}^- + 2S_m{}^zS_g{}^+S_g{}^- - 2S_g{}^zS_m{}^+S_m{}^-]. \quad \text{(A5h)}$$

To insure the accuracy of the above result, we have first taken the precaution of using the correct value for $\rho_g{}^{(2)}(t)$ to calculate $\rho_g{}^{(3)}(t)$. The accuracy of $\rho_g{}^{(2)}(t)$ is relatively easy to ascertain, both by double checking and by making sure that it yields the correct result for the fourth frequency moment $\langle\omega^4\rangle_{\mathbf{K}}$, when used in the form

$$\lim_{\beta\to 0}\langle\omega^4\rangle_{\mathbf{K}}=2\sum_{(g-w)} e^{-i\mathbf{K}(g-w)}\langle\rho_g{}^{(2)}(t)\rho_w{}^{(2)}(t')\rangle_{t=t'}. \quad \text{(A6)}$$

Similarly, the accuracy of $\rho_g{}^{(3)}(t)$ was ascertained by both double checking and also evaluating the fourth moment in the following fashion:

$$\lim_{\beta\to 0}\langle\omega^4\rangle_{\mathbf{K}}=-2\sum_{(g-w)} e^{-i\mathbf{K}(g-w)}\langle\rho_g{}^{(3)}(t)\rho_w{}^{(1)}(t')\rangle_{t=t'}. \quad \text{(A7)}$$

The identity of the results (A6) and (A7) and their exact agreement with the well-known corresponding results obtained by Marshall and co-workers (see Ref. 3 and other references cited therein) gives one confidence in the correctness of $\rho_g{}^{(3)}(t)$.

It should be mentioned here that the given form of $\rho_g{}^{(3)}(t)$ in Eqs. (4) and (5a)–(5b) was obtained after suitable additions and equivalent subtractions of spatial Kronecker delta functions in such a way that, when appropriate lattice summations are carried out, the result is zero if any of the spatial indices are the same. This is a great aid in taking traces of the form (A1), because we know that the various spatial indices then always refer to different sites within $\rho_g{}^{(3)}(t)$. The sixth moment now becomes

$$\langle\omega^6\rangle_{\mathbf{K}}=-2\sum_{(g-w)} e^{-i\mathbf{K}(g-w)}$$
$$\times\mathrm{Tr}[A_gA_w+B_gB_w+C_gC_w+D_gD_w+E_gE_w$$
$$+F_gF_w+H_gH_w+2C_gE_w+2F_gF_w]/\mathrm{Tr}(1). \quad \text{(A8)}$$

The traces of all the other terms (that the product $\rho_g{}^{(3)}\rho_w{}^{(3)}$ contains) are identically vanishing. Consider for example all possible terms involving A_g and B_g which contain spin operators of the form $S_f{}^zS_g{}^zS_i{}^+S_m{}^-$ and $S_f{}^+S_i{}^-S_g{}^+S_m{}^-$, respectively, where f, g, i, and m are all distinct. Since all of the other terms in the third derivative have at most three free (and distinct) indices, we have only to consider the terms $\mathrm{Tr}A_gA_w$, $\mathrm{Tr}B_gB_w$, and $\mathrm{Tr}2B_gA_w$, and the last of these is easily seen to be zero also.

In conclusion, it should be mentioned that the various quantum-mechanical traces that occur in the foregoing calculation have been tabulated in the literature.[6] In the present calculation, these tables were used without completely rechecking all the relevant traces.

[6] E. Ambler, J. C. Einstein, and J. F. Schooley, J. Math. Phys. **3**, 118 (1962).